Eur. Phys. J. D (2015) 69: 1
DOI: 10.1140/epjd/e2014-50648-6

THE EUROPEAN PHYSICAL JOURNAL D

Regular Article

Natural widths and blackbody radiation induced shift and broadening of Rydberg levels in magnesium ions*

Igor L. Glukhov[a], Sergey N. Mokhnenko, Elizaveta A. Nikitina, and Vitaly D. Ovsiannikov

Faculty of Physics, Voronezh State University, University square 1, 394006 Voronezh, Russia

Received 31 August 2014 / Received in final form 20 October 2014
Published online 8 January 2015 –

Abstract. Theoretical analysis is presented of the natural lifetimes and blackbody-radiation (BBR)-induced shifts and widths of Rydberg states with small and large angular momenta l. Asymptotic presentations in elementary functions are derived for matrix elements of bound-bound, bound-free and threshold radiative transitions from hydrogenic-type states with large angular momenta, applicable to both hydrogen-like and many-electron atoms and ions. For states with small angular momenta two numerical methods based on the quantum defects were used and corresponding data are compared with one another and with the most reliable data of the literature. Asymptotic approximations are derived for natural lifetimes, thermal shifts and broadening of Rydberg states of small and high l and principal quantum numbers $n \gg 1$.

1 Introduction

Intensive studies on the possibilities of the use of Rydberg states in practical applications have stimulated arising interest to detailed investigations into different optical properties of highly excited atoms and ions. The latest activities in a number of international research groups were concentrated on the alkaline-earth elements currently used as the most promising objects for designing new time-frequency standards based on high-precision measurements of optical and ultraviolet frequencies of transitions in atoms and ions [1–3]. Rydberg states of atoms/ions, as the most sensitive to external fields, may become useful tools for instant control of environmental characteristics, in order to reduce uncertainties of measurements to the lowest accessible level [4].

The most important quantities determining optical properties of Rydberg atoms and ions are natural lifetimes τ_{nl} and electromagnetic susceptibilities, first of all, the static $\alpha_{nl}(0)$ and dynamic (frequency-dependent) $\alpha_{nl}(\omega)$ dipole polarizabilities, which represent the principal quantitative characteristics of interaction between atom in its bound state $|nl\rangle$ and external field. Numerical values of static and dynamic polarizabilities determine the blackbody-radiation (BBR)-induced shifts of energy levels in the low-temperature ($kT \ll |E_{nl} - E_{n'l'}|$) and high-temperature ($kT \gg |E_{nl} - E_{n'l'}|$) environment, correspondingly (here k is the Boltzmann constant, which in atomic units is $k = 1/T_a = 3.1668 \times 10^{-6}$ a.u./K, where $T_a = 315\,776$ K is the atomic unit of temperature; T is the absolute temperature in Kelvin, $E_{nl} - E_{n'l'}$ is the energy of transition between nearest energy levels). It is important to note that $\alpha_{nl}(0)$ and $\alpha_{nl}(\omega)$ exhibit quite different behaviour as functions of the Rydberg-state principal quantum number n. The static polarizabilities are rapidly growing functions of n, $\alpha_{nl}(0) \propto n^7$ (see e.g. [5,6]), whereas the dynamic polarizability in the optical range of frequencies is approximately one and the same value for all Rydberg states, excluding only very narrow regions of resonances with lower-energy states.

In this article, we present detailed studies of the BBR-induced shifts and splitting of Rydberg levels in magnesium ions. The atomic system of units is used throughout the paper, $e = m = \hbar = 1$, unless otherwise specified explicitly. The unit atomic speed is $v_a = c/137.036$, where c is the speed of light. For convenience, the temperature is described only in Kelvin.

2 High-frequency polarizabilities of Rydberg states

The Rydberg-state dynamic polarizabilities determine energy shifts in a monochromatic electromagnetic wave. With the growth of principal quantum numbers these shifts gradually approach to their asymptotic values, corresponding to the energy of free-electron oscillations. At the frequencies, well exceeding the ionization potential of a Rydberg state $\omega/|E_{nl}| \equiv \Omega \gg 1$ and essentially smaller

* Contribution to the Topical Issue "Elementary Processes with Atoms and Molecules in Isolated and Aggregated States", edited by Friedrich Aumayr, Bratislav Marinkovic, Stefan Matejcik, John Tanis and Kurt H. Becker.

[a] e-mail: GlukhovOfficial@mail.ru

than the energy of two-electron excitations, the real part of scalar dynamic polarizability scales according to the law of inverse frequency squared, one and the same for all states, independently of quantum numbers [7–9]

$$\mathrm{Re}\{\alpha^{\mathrm{s}}_{nl}(\omega)\} \approx -\frac{1}{\omega^2}. \tag{1}$$

The imaginary part is determined by the photoionization cross section:

$$\mathrm{Im}\{\alpha^{\mathrm{s}}_{nl}(\omega)\} = \frac{c}{4\pi\omega}\sigma_{nl}(\omega), \tag{2}$$

which is a rapidly vanishing function of the frequency ω and the principal quantum number n. For Rydberg states with $l < 5$ (nS, nP, nD, nF, nG-states) the quasi-classical estimates [10] give $\sigma_{nl}(\omega) \approx \sigma^{\mathrm{thr}}_{nl}/\Omega^{7/3}$, where $\sigma^{\mathrm{thr}}_{nl} = \sigma_{nl}(\omega = |E_{nl}|)$ is the threshold cross section, for which also the WKB-approximation may be used [10,11]. The indicated dependencies demonstrate a rapid decrease of the imaginary part (2) with the increase of both the frequency and the principal quantum number,

$$\mathrm{Im}\{\alpha^{\mathrm{s}}_{nl}(\omega)\} \propto Z^{14/3} n^{-3} \omega^{-10/3}, \tag{3}$$

where Z is the charge of residual ion. Therefore, in the region of frequencies $\omega \gg |E_{nl}|$, the imaginary part of the Rydberg-state dynamic polarizability may be neglected in comparison with the real part (1). With the use of (1) and taking into account the rate of all BBR-stimulated transitions, an asymptotic expression for the shift $\varepsilon^{\mathrm{BBR}}_{nl}(T)$ and broadening $\Gamma^{\mathrm{BBR}}_{nl}(T)$ of Rydberg energy levels by the BBR of the temperature $kT \gg |E_{nl}|$ may be derived [12,13]

$$\begin{aligned} \Delta E^{\mathrm{BBR}}_{nl}(T) &= \varepsilon^{\mathrm{BBR}}_{nl}(T) - i\frac{\Gamma^{\mathrm{BBR}}_{nl}(T)}{2} \\ &\approx \frac{\pi}{3c^3}(kT)^2 - i\frac{2kT}{3c^2n^2}. \end{aligned} \tag{4}$$

Rigorously speaking, the free-electron approximation (1) is applicable to states with sufficiently high angular momenta ($l > 5$) and does not describe precisely polarizabilities of atomic states with low momenta, since it does not account for possible resonances with lower states of angular momenta $l' = l \pm 1$, the energy of transitions to which may be close to ω. Moreover, equation (1) holds if the interaction with core electrons of the residual ion does not influence significantly on the Rydberg-electron wave function. This interaction may be neglected for states with high angular momentum, repelled from the core by sufficiently strong centrifugal potential

$$U_c(r) = \frac{l(l+1)}{2r^2}. \tag{5}$$

The wave functions of low-angular-momentum states penetrate deeply inside the core and may be modified significantly, unlike the hydrogenic functions of high-l-states. That is why the asymptotic values of the frequency-dependent polarizability of states with $l < 5$ may differ from those of equation (1).

The asymptotic equations for the Rydberg-state dynamic polarizability and higher-order in $1/\omega^2$ corrections to the principal term (1) may be determined by reducing the infinite summations to the sum rules of oscillator strengths and their moments (see for example [8,9]), represented in terms of simple closed expressions [14,15]. In these sums the contribution of continuum is strongly dependent on the orbital momentum of the Rydberg state. This contribution may be significant for states with small momentum, whereas for large l (usually, for $l > 5$) it vanishes exponentially with the increase of the principal quantum number n.

3 Asymptotic features of natural widths, photoionization cross sections and BBR-induced shifts and broadening of states with high angular momenta

Detailed calculations of the shift and broadening of Rydberg-state energy levels in hydrogen, helium and alkali-metal atoms revealed noticeable departures from the asymptotic data, specifically for low-angular-momenta states, which in many-electron atoms have the largest quantum defects and therefore exhibit most clearly evident departures of optical properties from those of the hydrogenic states [16]. These departures were explained by contributions from the lower-energy states $|n'l'\rangle$ for which a relation holds $E_{nl} - E_{n'l'} > kT$, in contrast to the high-temperature asymptotic requirement for equation (4), $|E_{nl} - E_{n'l'}| \ll kT$. The separation of contributions from the lower- and upper-energy states (decays and excitations) into broadening of a low-momentum Rydberg state $|nl\rangle$ in hydrogen, helium and alkali atoms has demonstrated significant dependencies of these contributions on individual structures of the energy spectra in S-, P-, D-, F-series of states [17,18]. In addition, considerable contributions into shift and broadening come from continuum, which account for the BBR-induced ionization and the upward shifts of Rydberg levels. For the low-l states these contributions are overestimated in the asymptotic equations since the threshold ionization cross section σ^{thr}_{nl} increases with n approximately as $\sigma^{\mathrm{thr}}_{nl} \propto n^{5/3}$, while the above-threshold cross section rather smoothly decreases as a function of the BBR-photon frequency, approximately as [17,18]:

$$\sigma_{nl}(\omega) \approx \sigma^{\mathrm{thr}}_{nl}/\Omega^{7/3}. \tag{6}$$

For the low-momentum series of states, the use of asymptotic approximation (1), assumed to spread over all frequency range of the Planck's distribution from zero up to infinity, may either overestimate or underestimate the positive (upward) shift of the Rydberg-state energy by high-frequency thermal photons and the negative (downward) shift by low-frequency photons. In particular, the contributions of continuum are overestimated both in the level broadening [18], corresponding to the probability of BBR-induced ionization, and in the upward shift of energy.

The situation for high-l hydrogenic-type orbits ($10 < l \leq n-1$) is quite different. Here only a small number of states $|n'l'\rangle$ with $l' = l \pm 1$ and n' from $n' = l'+1$ to $n' = n-1$ remain below the state $|nl\rangle$. Evidently, the asymptotic condition $|E_{nl} - E_{n'l'}| \ll kT$ may hold for them automatically if the binding energy is significantly smaller than the thermal, $|E_{nl}| \ll kT$. In addition, the radial matrix elements of dipole transitions decrease with the increase of difference between principal quantum numbers $|n'-n|$ as $n^{-|n'-n|}$. Therefore the principal contribution to the spontaneous-decay rate $P^{\rm sp}_{nl}$ of high-l states comes from two closest states with $n' = n \pm 1$. The general behaviour of the natural lifetime τ^{sp}_{nl} of a state with high quantum numbers l and n may be presented as:

$$\tau^{\rm sp}_{nl} \approx \frac{t_0}{Z^4} n^3 l^2 u(n,l) \tag{7}$$

where $u(n,l) \xrightarrow[n>l\to\infty]{} 1$ is a dimensionless function, which adjusts the right-hand-side expression with exact values of $\tau^{\rm sp}_{nl}$ for arbitrary l and n, $t_0 \approx 0.0934$ nanoseconds is a constant value, independent of the Rydberg-state quantum numbers. Evidently, if the orbital quantum number is proportional to n, the rate of spontaneous decay vanishes following the law $P^{\rm sp}_{nl} \propto 1/n^5$, which is reduced by the factor n^{-2} in comparison with the rate $P^{\rm sp}_{nl} \propto 1/n^3$ for fixed-l states, for which the principal contribution to $P^{\rm sp}_{nl}$ comes from the rates of decay into the lowest dipole-connected states.

The ionization cross section for high-l states falls down exponentially with $n \gg 1$. For example, the cross section of the threshold ionization of a circular state, $l = n-1$, may be presented as:

$$\sigma^{\rm thr}_{n,l=n-1} = \frac{16\pi^{3/2} n^{5/2}}{3Z^2 c} \left(\frac{2}{e}\right)^{2n} \left(1 + \frac{1}{2n} + \frac{1}{2n^2} + o\left(\frac{1}{n^3}\right)\right). \tag{8}$$

The plot of the n-dependence of this function is given in Figure 1, where the logarithmic scale for the cross section is used in the vertical axis. Above the threshold, the frequency-dependent cross section $\sigma_{n,l=n-1}(\omega) = \sigma^{\rm thr}_{n,l=n-1} f_n(\omega)$ is also a decreasing function of frequency, as is seen from the rapidly vanishing factor,

$$f_n(\omega) = \frac{1}{\Omega^{5/2}} \left[\frac{\exp\left(1 - \arctan(\Omega-1)/\sqrt{\Omega-1}\right)}{\sqrt{\Omega}}\right]^{2n}. \tag{9}$$

Corresponding functions of the fractional frequency $\Omega = \omega/|E_{nl}|$ are presented in Figure 2 for the circular states of $n = 10, 30, 50$.

So, the principal contribution to the BBR-induced depopulation rate for high-l Rydberg states comes from transitions to the closest upper and lower states with $n' = n \pm 1$. Besides that, the high-l states in all atoms are hydrogen-like, without any quantum defects. Therefore, the single-electron sum rules for them hold with high precision, together with asymptotic equations (1) and (2) for the frequency-dependent polarizability (there are no resonant states in the lower region of energy) and equation (4)

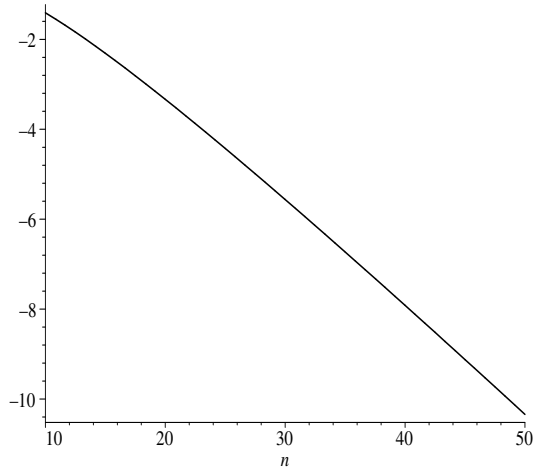

Fig. 1. The threshold ionization cross section (8) of circular states with $l = n-1$ as a function of the principal quantum number n. The logarithmic scale $\log(\sigma^{\rm thr}_{n,l=n-1})$ is presented in the vertical axis.

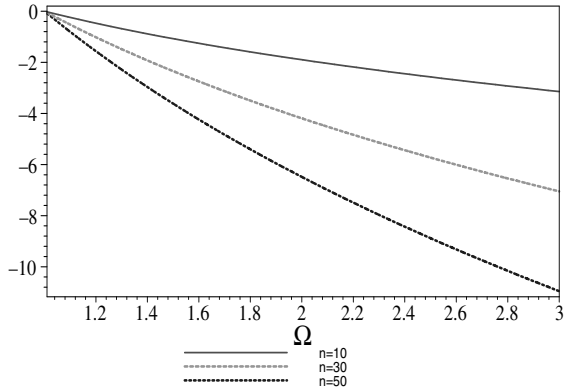

Fig. 2. Dependence on the normalized frequency $\Omega = \omega/|E_{nl}|$ of the fractional photoionization cross sections (9) for circular Rydberg states. The logarithmic scale, $\log(f_n(\omega))$, is given in the vertical axis.

for the BBR-induced shift and broadening. It should also be noted that the contribution of continuum for high-l states is negligibly small.

4 Asymptotic features of natural widths, photoionization cross-sections and BBR-induced shifts and broadening of states with low angular momenta

The basic optical characteristics for the low-l states in many-electron atoms may differ significantly from those described above. In particular, due to a more rapid spontaneous decay, the natural lifetimes and corresponding line widths exceed those of the high-l states. In addition, the cross sections of photoionization from the low-l states do not vanish exponentially. Moreover, the threshold ionization cross section grows up together with the principal quantum number as $\sigma^{\rm thr}_{nl} \propto n^{5/3}$ [10] and in

Table 1. Numerical values of parameters B_l of the potential (10) and corresponding effective orbital momenta λ_l for S-, P-, D- and F-series of Rydberg states in Mg^+ ions.

Series	$S_{1/2}$	$P_{1/2}$	$P_{3/2}$	$D_{3/2}$	$D_{5/2}$	$F_{5/2,7/2}$
B_l	−0.0319	0.4969	0.4992	−0.1113	−0.1113	−0.01163
λ_l	−0.0686	1.3011	1.3024	1.955	1.995	2.997

the above-threshold region it does not decrease exponentially with frequency, but follows the power law (6). The dynamic polarizabilities of the low-l states for the bulk of the BBR frequencies experience significant departures from the asymptotic law (1). In addition, the Rydberg states with $l < 5$ in many-electron atoms have significant quantum defects which can modify the oscillator-strength sum rules. Therefore, the results of calculations based on different approximations to the radial wave functions of the low-angular-momentum states may differ significantly. We consider two methods which use quantum defects for modifications of the Coulomb (hydrogenic) radial wave functions for describing the single-electron wave function in a many-electron atom: (i) the quantum defect method (QDM) [19] and (ii) the fues' model potential (FMP) approximation [20–22]. The both approaches deal with one and the same object and modify the Coulomb wave function so as to take into account the exact single-electron spectrum of energies. To this end, the non-integer effective principal quantum number (PQN) $\nu_{nl} = Z/\sqrt{-2E_{nl}}$ is introduced instead of the integer PQN n at the cost of singularity of the wave function in the origin in the QDM approach and at the cost of introduction of the non-integer angular momentum

$$l \to \lambda = \sqrt{(l+1/2)^2 + 2B_l} - 1/2 \neq l$$

in the FMP approximation. The parameters B_l, determining the non-Coulomb part of the FMP

$$V_F(\boldsymbol{r}) = -\frac{Z}{r} + \sum_{l=0}^{\infty} \frac{B_l}{r^2} \sum_{m=-l}^{l} \hat{P}_{lm}(\theta,\phi), \qquad (10)$$

may impart significant deviations to the centrifugal potential (5) and to the corresponding radial wave functions of the external-electron states. Evidently, the largest absolute values of B_l correspond to states with low l, whereas they vanish for $l \gg 1$, so that in most cases $B_l = 0$ already for $l > 5$ (see, for example, Table 1 for S-, P-, D-, F-states in Mg^+ ions).

In the use of the QDM also some difficulties and restrictions appear in the case of low-l states. In particular, the QDM becomes inapplicable to describing wave functions of low-energy states with angular momentum $l > \nu_{nl}$ (np^6 ground states of inert atoms, the lowest nd-states in alkaline-earth atoms and ions, etc.). Similar difficulties, caused by significant departures of the model potential (10) from the really existing centrifugal potential (5) inside the atomic core, may appear in the FMP approach for states with $|\lambda - l| > 1$ [23]. The most spectacular manifestation of these difficulties is the departure of the dipole-transition oscillator strengths $2\omega_{n'l'nl}|\langle n'l'|z|nl\rangle|^2$, determined by the FMP wave functions of such states, from the most reliable data of the literature (z is the component of the valence-electron position vector). These departures cause corresponding deviations from the Thomas-Reiche-Kuhn sum rules. This effect is due to the second term of the potential (10) with the sum of projection operators $\hat{P}_{lm}(\theta,\phi) = |Y_{lm}(\theta,\phi)\rangle\langle Y^*_{lm}(\theta,\phi)|$, where the integration is implied over the angular variables θ, ϕ of the position vector $\boldsymbol{r}$. This non-local operator does not commute with the operator of dipole moment and introduces corresponding corrections to the sum rules:

$$S_{nl}(q) = \sum_{n'l'} 2\omega^{1+q}_{n'l',nl}|\langle n'l'|z|nl\rangle|^2. \qquad (11)$$

So, for the basic sum rule, $q = 0$, which in the single-electron approximation should equal unity, the wave-functions of the FMP approach give:

$$S_{nl}(0) = 1 + \frac{2}{3(2l+1)}\left[lB_{l-1} + (l+1)B_{l+1} - (2l+1)B_l\right]. \qquad (12)$$

This sum appears in the asymptotic value of the BBR-induced shift (the real part of Eq. (4)). The asymptotic value of BBR-induced broadening (the imaginary part of Eq. (4)) involves the sum $q = 1$, which also includes the corrections appearing from the non-local part of the FMP (10):

$$S_{nl}(1) = \frac{Z^2}{3\nu^2_{nl}}\left[1 + \frac{l(B_l - B_{l-1})^2 + (l+1)(B_l - B_{l+1})^2}{(2l+1)(\lambda_l + 1/2)\nu_{nl}}\right]. \qquad (13)$$

However, the correction, determined in equation (13) by the fraction in the brackets, gradually decreases with the increase of the effective quantum number of the Rydberg state ν_{nl} and becomes negligibly small for sufficiently high energy levels.

5 Natural widths and BBR-induced shifts and broadening of Rydberg states in Mg^+ ions

In calculating BBR-induced shifts of Rydberg levels of small angular momenta with the use of the FMP approach, the results may differ considerably from the asymptotic values of equation (4). Nevertheless, for imaginary parts of the shift (4), determining the broadening of high-energy Rydberg states ($\nu_{nl} \gg 1$), the corrections disappear as is seen from the data for the coefficients B_l of the FMP (10) presented in Table 1 and used in equation (13). Therefore the data for the natural widths and BBR-induced broadening may be rather reliably determined in the FMP approximation.

Table 2. Numerical values of constants $b_{ik}^{\mathrm{dec(exc)}}$ of the temperature-dependent polynomials determining the coefficients (19) of the asymptotic presentations (17) for the fractional rates of the BBR-induced radiation decays and excitations from Rydberg nP-states of Mg^+ ions.

i	b_{i0}^{dec}	b_{i1}^{dec}	b_{i2}^{dec}	b_{i0}^{exc}	b_{i1}^{exc}	b_{i2}^{exc}
0	129.96	−20.83	21.32	391.24	−56.77	63.42
1	−46.62	125.27	−133.8	−645.2	1108.8	−744.8
2	−150.5	263.5	−28.36	307.0	−873.5	682.9

From the FMP-data for spontaneous radiation-decay rates of the nS Rydberg states $\Gamma_{nS}^{\mathrm{sp}}$ in Mg^+ ions, the asymptotic equation was derived for the natural lifetimes which is well consistent with the data of the literature and reproduces with a good precision the results of calculations in the QDM:

$$\tau_{nS}^{\mathrm{sp}} = 0.063914n^3\left(1-\frac{3.22}{n}+\frac{6.46}{n^2}-\frac{0.367}{n^3}\right),\ \mathrm{ns}. \quad (14)$$

The asymptotic approximation for the lifetime of nP-states may be written as:

$$\tau_{nP}^{\mathrm{sp}} = 1.59894n^3\left(1-\frac{2.394}{n}-\frac{56.42}{n^2}+\frac{342.5}{n^3}\right),\ \mathrm{ns}. \quad (15)$$

Evidently, the nP-states live about 20−30 times longer than the states of nS-series.

The BBR-induced broadening of the nl-states includes three separate kinds of transitions. One of them corresponds to the rate of BBR-stimulated downward transitions (decays) $\Gamma_{nl}^{\mathrm{dec}}(T)$, which is temperature-dependent and conveniently described by the fractional rate of decays $R_{nl}^{\mathrm{dec}} = \Gamma_{nl}^{\mathrm{dec}}/\Gamma_{nl}^{\mathrm{sp}}$. The two remaining are the upward BBR-supported transitions: excitations of the upper bound levels determined by the fractional rate of excitations $R_{nl}^{\mathrm{exc}} = \Gamma_{nl}^{\mathrm{exc}}/\Gamma_{nl}^{\mathrm{sp}}$, and BBR-induced transitions into continuum, which is also determined by the fractional rate of ionization $R_{nl}^{\mathrm{ion}} = \Gamma_{nl}^{\mathrm{ion}}/\Gamma_{nl}^{\mathrm{sp}}$. Thus, the total nS-level broadening may be determined as:

$$\Gamma_{nl}^{\mathrm{BBR}}(T) = \Gamma_{nl}^{\mathrm{sp}}\left(R_{nl}^{\mathrm{dec}}+R_{nl}^{\mathrm{exc}}+R_{nl}^{\mathrm{ion}}\right). \quad (16)$$

The separate terms in parenthesis are temperature dependent and in the asymptotic region $|E_{nl}| \ll kT$ are directly proportional to T. However, the dependence on the principal quantum number of $R_{nl}^{\mathrm{ion}}(T)$ differs from those of $R_{nl}^{\mathrm{dec(exc)}}(T)$, at least for the low-$l$ states [18]. This effect comes from different energy separations between states providing principal contributions to the three processes. Therefore, the rates of decays and excitations may be described by one and the same asymptotic interpolation equation:

$$R_{nl}^{\mathrm{dec(exc)}}(T) = \frac{a_0^{\mathrm{dec(exc)}}(T)+a_1^{\mathrm{dec(exc)}}(T)x+a_2^{\mathrm{dec(exc)}}(T)x^2}{n^2\left[\exp\left(\frac{Z^2T_a}{n^3T}\right)-1\right]}$$
$$x = \frac{100}{nT^{1/3}} \quad (17)$$

whereas the fractional rate of ionization is approximated by the equation

$$R_{nl}^{\mathrm{ion}}(T) = \frac{a_0^{\mathrm{ion}}+a_1^{\mathrm{ion}}y+a_2^{\mathrm{ion}}y^2}{n^p\left[\exp\left(\frac{Z^2T_a}{2n^2T}\right)-1\right]},$$
$$y = \frac{100}{nT^{1/2}} \quad (18)$$

where the exponent $p = 4/3$ for states $l \neq 0$. For nS-states the fitting procedures fix different values of p starting from 1/4 to 3/4 in different regions of n. The smooth dependence on the temperature of the coefficients $a_i^{\mathrm{dec(exc,ion)}}(T)$ may also be polynomial-approximated, as follows:

$$a_i^{\mathrm{dec(exc)}}(T) = \sum_{k=0}^{2} b_{ik}^{\mathrm{dec(exc)}}t^k, \quad t = \left(\frac{100}{T}\right)^{1/3} \quad (19)$$

$$a_i^{\mathrm{ion}}(T) = \sum_{k=0}^{2} b_{ik}^{\mathrm{ion}}\tau^k, \quad \tau = \left(\frac{100}{T}\right)^{1/2}. \quad (20)$$

The coefficients b_{ik} are constant values, independent of n and T, determined by fitting the calculated data for the fractional rates of BBR-induced decays, excitations and ionization of sufficiently high Rydberg states of the series nl. Numerical values of the coefficient for nP-states in Mg^+ ions are presented in Tables 2 and 3. These values may be used in equations (16)–(20) to reproduce calculated data for the BBR-induced broadening with an error below 3% for nP-states with their principal quantum numbers in the region of $n > 10$ and temperatures $T > 100$ K.

Figures 3 and 4 present the numerical data for the fractional rates $R_{nP}^{\mathrm{exc}}(T)$ of BBR-induced excitations from nP-states into higher-energy $n'S$- and $n'D$-states, as functions of the temperature and principal quantum numbers. Figures 5 and 6 give corresponding dependencies of the fractional rates of BBR-induced decays $R_{nP}^{\mathrm{dec}}(T)$. The data of straightforward calculations (presented in symbols) according to general equations for the BBR-induced effects on Rydberg-state energy levels [12,13,16,18] is compared with the data of approximation equations (17) and (19) (presented in lines). The departure between exact and approximate results does not exceed 1% in T- and n-regions presented in the plots. A remarkable correlation of the data for response to the BBR of the Rydberg-state magnesium ions with highly excited neutral sodium atoms [18] should be mentioned. Firstly, both in Na atoms and

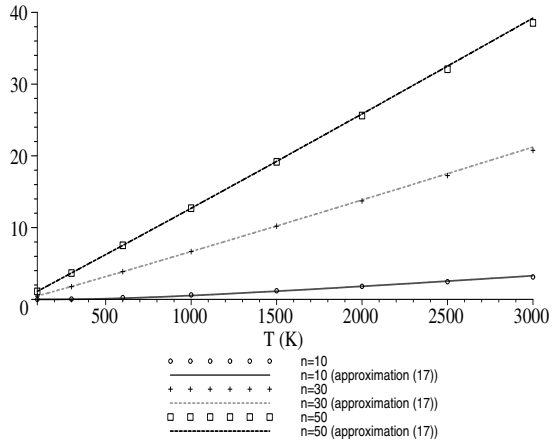

Fig. 3. Dependence on the temperature T of the fractional BBR-induced excitation rates $R^{\rm exc}_{nP}$ of equation (17) (lines) for Rydberg nP-states of the principal quantum numbers $n = 10$, 30, 50 in comparison with exactly calculated data (symbols).

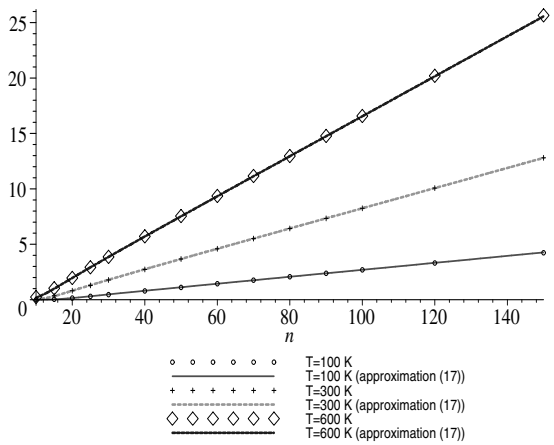

Fig. 4. Dependence on the principal quantum number n of the fractional BBR-induced excitation rates $R^{\rm exc}_{nP}$ of equation (17) (lines) for Rydberg nP-states of magnesium ions at the BBR temperatures $T = 100$, 300 and 600 K, in comparison with exactly calculated data (symbols).

Mg^+ ions, the rates of Rydberg nS-state spontaneous decays exceed more than one order those of nP-states. Secondly, the fractional rates of BBR-induced excitations of nP-states more than twice exceeds the fractional rates of BBR-induced decays (as is seen from numerical values of coefficients $b^{\rm dec(exc)}_{00}$ of Table 2. So, in Mg^+: $R^{\rm exc}_{nP}(T) \approx 3R^{\rm dec}_{nP}(T)$).

The real part of the shift (4) may also be approximated asymptotically as (in Hertz)

$$\varepsilon^{\rm BBR}_{nl}(T) = 2416.6 \left(\frac{T}{300}\right)^2 \left(a^\varepsilon_0(T) + a^\varepsilon_1(T)z + a^\varepsilon_2(T)z^2\right)$$
$$z = \left|\frac{E_{nl}}{kT}\right|^{1/2} \qquad (21)$$

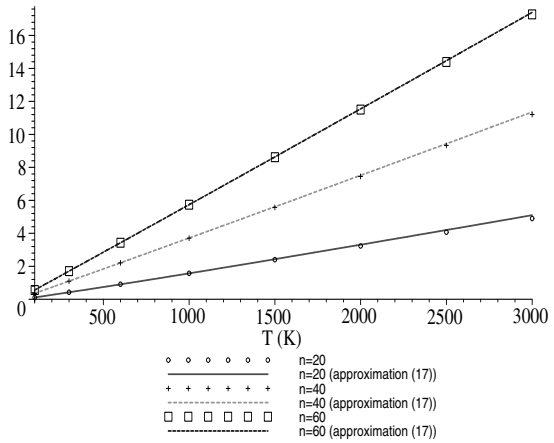

Fig. 5. Dependence on the temperature T of the fractional BBR-induced decay rates $R^{\rm dec}_{nP}$ of equation (17) (lines) in comparison with exactly calculated data (symbols) for Rydberg nP-states of the principal quantum numbers $n = 20$, 40, 60 in magnesium ions.

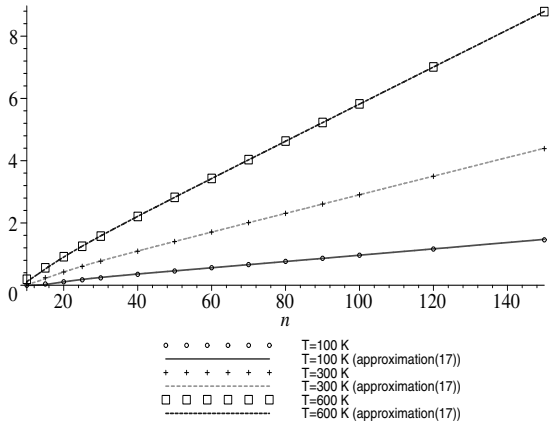

Fig. 6. Dependence on the principal quantum number n of the fractional BBR-induced decay rates $R^{\rm dec}_{nP}$ of equation (17) (lines) in comparison with exactly calculated data (symbols) for Rydberg nP-states of magnesium ions at the BBR temperatures $T = 100$, 300 and 600 K.

with coefficients smoothly dependent on the temperature, similar to (19) and (20):

$$a^\varepsilon_i = \sum_{k=0}^{2} b^\varepsilon_{ik}\tau^k, \quad \tau = \left(\frac{100}{T}\right)^{1/2}. \qquad (22)$$

The coefficients b^ε_{ik} are constant values for each nl-series of states. The most important of them $b^\varepsilon_{00} = 1$ is one and the same for all series of Rydberg states and determines the asymptotic for $n \to \infty$ value $\varepsilon^{\rm BBR}_{nl}(T = 300\ {\rm K}) = 2416.6$ Hz of the BBR-induced shift of highly excited states [16]. However, this value assumes the oscillator-strengths sum rule be equal to the unity. However, the FMP wavefunctions do not hold this condition, as follows from equation (12). Therefore we used the wavefunctions of the quantum defect method (QDM) to calculating dipole matrix elements for radiation transitions. Numerical data of these calculations of constants b^ε_{ik} are presented in Table 3.

Table 3. Numerical values of constants $b_{ik}^{\mathrm{ion}(\varepsilon)}$ of the temperature-dependent polynomials determining the coefficients (20) of the asymptotic presentations (18) and (21), (22) for the rates of the BBR-induced ionization and shifts of Rydberg nP-states of Mg^+ ions.

i	b_{i0}^{ion}	b_{i1}^{ion}	b_{i2}^{ion}	b_{i0}^{ε}	b_{i1}^{ε}	b_{i2}^{ε}
0	157.6	−66.62	5.372	0.95356	0.03068	−0.08752
1	−2529	3450	−1532	−0.05568	0.19402	0.08467
2	12612	−25180	13580	0.01254	−0.33272	0.08404

This work was supported by the Ministry of Education and Science of Russia in the framework of the state order on research activities in 2014–2016 (Project No. 1226) and by the Russian Foundation for Basic Research (RFBR Grant No. 14-02-00516-a).

References

1. T. Rosenband et al., Science **319**, 1808 (2008)
2. N. Hinkley et al., Science **341**, 1215 (2013)
3. B.J. Bloom, T.L. Nicholson, J.R. Williams, Nature **506**, 71 (2014)
4. V.D. Ovsiannikov, A. Derevianko, K. Gibble, Phys. Rev. Lett. **107**, 093003 (2011)
5. Z.-C. Yan, Phys. Rev. A **62**, 052502 (2000)
6. E.Yu. Il'inova, A.A. Kamenski, V.D. Ovsiannikov, J. Phys. B **42**, 145004 (2009)
7. N.L. Manakov, V.D. Ovsiannikov, L.P. Rapoport, Phys. Rep. **141**, 319 (1986)
8. V.A. Davydkin, V.D. Ovsiannikov, B.A. Zon, Laser Phys. **3**, 449 (1993)
9. A.A. Krylovetsky, N.L. Manakov, S.I. Marmo, J. Phys. B **38**, 311 (2005)
10. N.B. Delone, S.P. Goreslavsky, V.P. Krainov, J. Phys. B **27**, 4403 (1994)
11. V.D. Ovsiannikov, I.L. Glukhov, E.A. Nekipelov, J. Phys. B **45**, 095003 (2012)
12. T.F. Gallagher, W.E. Cooke, Phys. Rev. Lett. **42**, 835 (1979)
13. W.E. Cooke, T.F. Gallagher, Phys. Rev. A **21**, 588 (1980)
14. H.S. Bethe, E.E. Salpeter, *Quantum Mechanics of One- and Two-Electron Atoms* (Springer, New York, 1957)
15. U. Fano, J.W. Cooper, Rev. Mod. Phys. **40**, 441 (1968)
16. J.W. Farley, W.H. Wing, Phys. Rev. A **23**, 2397 (1981)
17. I.L. Glukhov, E.A. Nekipelov, V.D. Ovsiannikov, J. Phys. B **43**, 125002 (2010)
18. V.D. Ovsiannikov, I.L. Glukhov, E.A. Nekipelov, J. Phys. B **44**, 195010 (2011)
19. D.R. Bates, A Damgaard, Philos. Trans. R. Soc. London A **242**, 101 (1949)
20. G. Simons, J. Chem. Phys. **55**, 756 (1971)
21. G. Simons, J. Chem. Phys. **60**, 645 (1974)
22. G. Simons, J. Chem. Phys. **62**, 4799 (1975)
23. A. Derevianko, W.R. Johnson, V.D. Ovsiannikov, V.G. Pal'chikov, D.R. Plante, G. von Oppen, J. Exp. Theor. Phys. **88**, 272 (1999)